

# Chapter 15

## Advanced electron transport algorithms

In this chapter we consider the transport of electrons in a condensed history Class II scheme [Ber63]. That is to say, the bremsstrahlung processes that result in the creation of photons above an energy threshold  $E_\gamma$ , and Møller knock-on electrons set in motion above an energy threshold  $E_\delta$ , are treated discretely by creation and transport. Sub-threshold processes are accounted for in a continuous slowing down approximation (CSDA) model. For further description of the Class II scheme the reader is encouraged to read Berger's article [Ber63] who coined the terminology and gave a full description and motivation for the classification scheme. Figure 15.1 gives a graphical description of the transport.

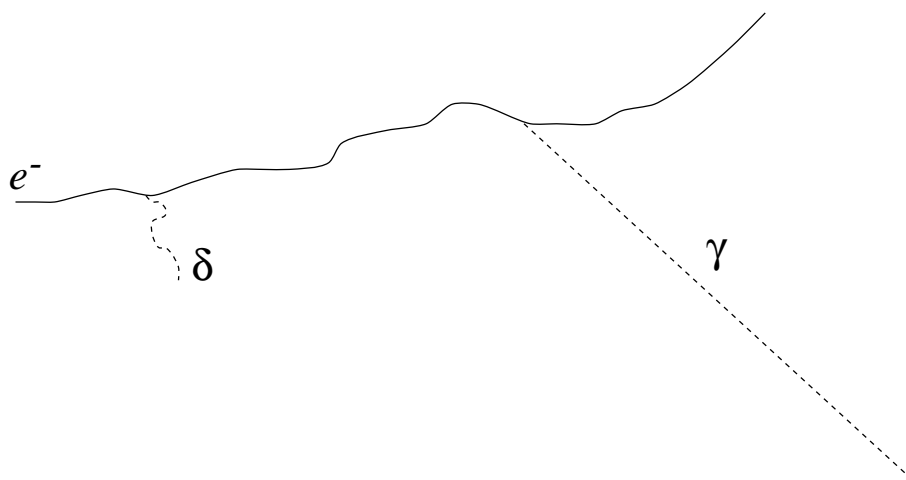


Figure 15.1: This is a depiction of a complete electron history showing elastic scattering, creation of bremsstrahlung above the  $E_\gamma$  threshold, the setting in motion of a knock-on electron above the  $E_\delta$  threshold and absorption of the primary and knock-on electrons.

The electron transport processes between the particle creation, absorption vertices is governed by the Boltzmann transport equation as formulated by Larsen [Lar92]:

$$\left[ \frac{1}{v} \frac{\partial}{\partial t} + \vec{\Omega} \cdot \vec{\nabla} + \sigma_s(E) - \frac{\partial}{\partial E} L(E) \right] \psi(\vec{x}, \vec{\Omega}, E, t) = \int_{4\pi} d\Omega' \sigma_s(\vec{\Omega} \cdot \vec{\Omega}', E) \psi(\vec{x}, \vec{\Omega}', E, t) , \quad (15.1)$$

where  $\vec{x}$  is the position,  $\vec{\Omega}$  is a unit vector indicating the direction of the electron,  $E$  is the energy of the electron and  $t$  is time.  $\sigma_s(\vec{\Omega} \cdot \vec{\Omega}', E)$  is the macroscopic differential scattering cross section,

$$\sigma_s(E) = \int_{4\pi} d\Omega' \sigma_s(\vec{\Omega} \cdot \vec{\Omega}', E) \quad (15.2)$$

is the total macroscopic cross section (probability per unit length),  $L(E)$  is the restricted stopping power appropriate for bremsstrahlung photon creation and Møller electrons beneath their respective thresholds  $E_\gamma$  and  $E_\delta$ ,  $v$  is the electron speed and  $\psi(\vec{x}, \vec{\Omega}, E, t) d\vec{x} d\Omega dE$  is the probability of there being an electron in  $d\vec{x}$  about  $\vec{x}$ , in  $d\Omega$  about  $\vec{\Omega}$  and in  $dE$  about  $E$  at time  $t$ . The boundary condition to be applied to each segment in Figure 15.1 is:

$$\psi(\vec{x}, \vec{\Omega}, E, 0) = \delta(\vec{x}) \delta(\hat{z} - \vec{\Omega}) \delta(E_n - E) , \quad (15.3)$$

where the start of each segment is translated to the origin and rotated to point in the  $z$ -direction. ( $\hat{z}$  is a unit vector pointing along the  $z$ -axis.) The energy at the start of the  $n$ -th segment is  $E_n$ .

For our considerations within the CSDA model, we note that  $E$  and  $t$  can be related since the pathlength,  $s$ ,

$$s = vt = \int_E^{E_n} \frac{dE'}{L(E')} , \quad (15.4)$$

permitting a slight simplification of Eq. 15.1:

$$\left[ \frac{\partial}{\partial s} + \vec{\Omega} \cdot \vec{\nabla} + \sigma_s(E) \right] \psi(\vec{x}, \vec{\Omega}, s) = \int_{4\pi} d\Omega' \sigma_s(\vec{\Omega} \cdot \vec{\Omega}', E) \psi(\vec{x}, \vec{\Omega}', s) . \quad (15.5)$$

The cross section still depends on  $E$  which may be calculated from Eq. 15.4.

Lewis [Lew50] has presented a “formal” solution to Eq.15.5. By assuming that  $\psi$  can be written in an expansion in spherical harmonics,

$$\psi(\vec{x}, \vec{\Omega}, s) = \sum_{lm} \psi_{lm}(\vec{x}, s) Y_{lm}(\vec{\Omega}) , \quad (15.6)$$

one finds that

$$\left[ \frac{\partial}{\partial s} + \kappa_l \right] \psi_{lm}(\vec{x}, s) = - \sum_{\lambda\mu} \vec{\nabla} \psi_{\lambda\mu}(\vec{x}, s) \cdot \vec{Q}_{lm}^{\lambda\mu} , \quad (15.7)$$

where

$$\kappa_l(E) = \int_{4\pi} d\Omega' \sigma_s(\vec{\Omega} \cdot \vec{\Omega}', E) [1 - P_l(\vec{\Omega} \cdot \vec{\Omega}')] , \quad (15.8)$$

and

$$\vec{Q}_{lm}^{\lambda\mu} = \int_{4\pi} d\Omega Y_{lm}^*(\vec{\Omega}) \vec{\Omega} Y_{\lambda\mu}(\vec{\Omega}) . \quad (15.9)$$

If one considers angular distribution only, then one may integrate over all  $\vec{x}$  in Eq. 15.7 giving:

$$\left[ \frac{\partial}{\partial s} + \kappa_l \right] \psi_l(s) = 0 , \quad (15.10)$$

resulting in the solution derived by Goudsmit and Saunderson [GS40a, GS40b]:

$$\psi(\vec{\Omega}, s) = \frac{1}{4\pi} \sum_l (2l+1) P_l(\hat{z} \cdot \vec{\Omega}) \exp\left(-\int_0^s ds' \kappa_l(E)\right) . \quad (15.11)$$

Eq. 15.7 represents a complete formal solution of the Class II CSDA electron transport problem but it has never been solved exactly. However, Eq. 15.7 may be employed to extract important information regarding the moments of the distributions. Employing the definition,

$$k_l(s) = \exp\left(-\int_0^s ds' \kappa_l(E)\right) , \quad (15.12)$$

Lewis [Lew50] has shown the moments  $\langle z \rangle$ ,  $\langle z \cos \Theta \rangle$ , and  $\langle x^2 + y^2 \rangle$  to be:

$$\langle z \rangle = \int_0^s ds' k_1(s') , \quad (15.13)$$

$$\langle z \cos \Theta \rangle = \frac{k_1(s)}{3} \int_0^s ds' \frac{1 + 2k_2(s')}{k_1(s')} , \quad (15.14)$$

and

$$\langle x^2 + y^2 \rangle = \frac{4}{3} \int_0^s ds' k_1(s') \int_0^{s'} ds'' \frac{1 - k_2(s'')}{k_1(s'')} . \quad (15.15)$$

It can also be shown using Lewis's methods that

$$\langle z^2 \rangle = \frac{2}{3} \int_0^s ds' k_1(s') \int_0^{s'} ds'' \frac{1 + 2k_2(s'')}{k_1(s'')} , \quad (15.16)$$

and

$$\langle x^2 + y^2 + z^2 \rangle = 2 \int_0^s ds' k_1(s') \int_0^{s'} ds'' \frac{1}{k_1(s'')} , \quad (15.17)$$

which gives the radial coordinate after the total transport distance,  $s$ . Note that there was an error<sup>1</sup> in Lewis's paper where the factor 1/3 was missing from his version of  $\langle z \cos \Theta \rangle$ . In the

---

<sup>1</sup>The correction of Lewis's Eq. 26 is:

$$H_{l1} = \sqrt{\frac{1}{4\pi(2l+1)}} k_l(s) \int_0^s ds' \frac{lk_{l-1}(s') + (l+1)k_{l+1}(s')}{k_1(s')}$$

The reader should consult Lewis's paper [Lew50] for the definition of the  $H$ -functions.

limit that  $s \rightarrow 0$ , one recovers from Eqs. 15.14 and 15.16 the results  $\lim_{s \rightarrow 0} \langle z \cos \Theta \rangle = s$  and  $\lim_{s \rightarrow 0} \langle z^2 \rangle = s^2$  which are not obtained without correcting the error as described in the footnote. Similar results for the moments have been derived recently by Kawrakow [Kaw96a] using a statistical approach.

Before leaving this introductory section it warrants repeating that these equations are all “exact” within the CSDA model and are independent of the form of the elastic scattering cross section. It should also be emphasized that Larsen analysis [Lar92] proves that the condensed history always gets the correct answer (consistent with the validity of the elastic scattering cross section) in the limit of small step-size providing that the “exact” Goudsmit-Saunderson multiple-scattering formalism is employed (and that its numerical stability problems at small step-size can be solved). Larsen analysis also draws some conclusions about the underlying Monte Carlo transport mechanisms and how they relate to convergence of results to the correct answer. Some Monte Carlo techniques can be expected to be less step-size dependent than others and converge to the correct answer more efficiently, using larger steps.

The ultimate goal of a Monte Carlo transport algorithm should be to make electron condensed history calculations as stable as possible with respect to step-size. That is, for a broad range of applications there should be step-size *independence* of the result. Hence, it would be most efficient to use steps as large as possible and not be subject to calculation errors. While we have not yet achieved this goal, we have made much progress towards it and describe some of this progress in a later section.

## 15.1 What does condensed history Monte Carlo do?

Monte Carlo calculations attempt to solve Eq. 15.5 iteratively by breaking up the transport between discrete interaction vertices, as depicted in Figure 15.2. The first factor determining the electron step-size distance is the distance to a discrete interaction. These distances are stochastic and characterized by an exponential distribution. Further subdivision schemes may be employed and these can be classified as numeric, physics’ or boundary step-size constraints.

### 15.1.1 Numerics’ step-size constraints

A geometric restriction, say  $s \leq s_{\max}$  may be used. A geometric restriction of this form was introduced by Rogers [Rog84b] in the EGS Monte Carlo code [NHR85, BHR94]. This has application in graphical displays of Monte Carlo histories. One wants the electron tracks to have smooth lines and so the individual pathlengths should be of the order of the resolution size of the graphics display. Otherwise, the tracks look artificially jagged, as they do in Figure 15.2. Of course, there are some real sharp bends in the electron tracks associated with large angle elastic scattering, but these are usually infrequent. One can predict the

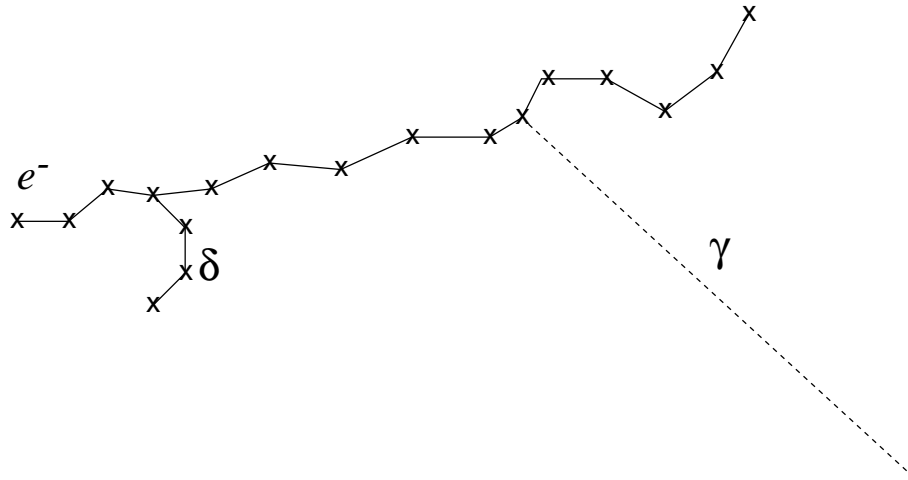


Figure 15.2: This is how a Monte Carlo calculates of the complete electron history as depicted in Figure 15.1. The transport takes place in steps, the vertices of which are marked with the symbol “x”.

number of steps required to follow a particle to termination. For this case  $N = r(E_i)/s_{\max}$ , where  $r(E_i)$  is the range of an electron with starting energy  $E_i$ .

Another popular choice is a constant fractional energy loss per electron step, *i.e.*  $\Delta E/E = \text{constant}$ . This has a slight disadvantage that the electron steps get shorter and shorter as the energy of the electrons in the simulation gets smaller and smaller. In terms of the dynamic range of the energies of the particles in the simulation, generally the lower ones play a lesser important role (there are exceptions to this of course!) and so, despite its popularity, it is probably wasteful in many applications. One can predict the number of steps required to follow a particle to termination in this case as well. For this case  $N = \log(1 - \Delta E/E)/\log(E_{\min}/E_i)$  where  $E_{\min}$  is the minimum electron energy for which transport takes place. One sees that as  $E_{\min}$  is pushed downwards by the requirements of some applications, that the number of steps acquires a slow logarithmic growth, unlike the geometric restriction. The constant fractional energy loss per electron step is built into the ETRAN Monte Carlo code [Ber63, Sel89, Sel91] and its well-known progeny, the ITS system [HKM<sup>+</sup>92] and the electron component of MCNP [Bri86, Bri93]. In these code systems, the value of the constant is kept in internal tables and its value determined through trial and error. In the EGS system [NHR85, BHNR94], it is available to the user as a “tuning” parameter, to be adjusted (lowered) until the answer converges to the (presumably correct) result.

There are other schemes of step-size restriction that will not be discussed. However, we see that the two discussed thus far play the role of an “integration mesh-density”. To get better results one must increase the resolution. To be practical, the mesh density ought to be as large as possible, consistent with target accuracy of the application. Larsen [Lar92] has made an interesting analysis of Monte Carlo algorithms and how they should be expected

to converge. He showed that the ETRAN scheme proposed by Berger [Ber63] contains  $O(\Delta s)$  errors. Thus, one expects that accurate calculation with ETRAN methods would converge slowly and require small step-sizes to get the answer correct. Indeed, this was the case with the EGS code as well, motivating the step-size restrictions introduced into EGS by Rogers [Rog84b].

Larsen [Lar92] also proposed an alternative Monte Carlo method (calling it “Method 3”) to enable faster convergence since it contains  $O(\Delta s^2)$  errors. The algorithm for each sub-step,  $\Delta s$ , is that first it must be broken into two parts. The first part is a drift of length  $\Delta s/2$  in the initial direction of motion, and a deduction in energy due to continuous energy losses over the first part of this step. The multiple-scattering angle is sampled at this new energy but for a deflection angle assuming that the particle as gone the full sub-step distance,  $\Delta s$ , and deflection by this angle. The sub-step is then completed by executing a drift of distance  $\Delta s/2$  in the new direction. Although this method may seem as if is doubling the number of steps, this is actually not the case since the most computer-intensive part of the process, namely sampling the multiple-scattering angle and rotation, is performed only once per sub-step.

The result of the “Method 3” procedure is to impart longitudinal and lateral distributions to the sub-step, both correlated to the multiple-scattering angle,  $\Theta$ . Assuming the particle starts at the origin and is directed along the  $z$ -axis, after a total sub-step pathlength of  $\Delta s$ , the final resting place will be:

$$\begin{aligned}\Delta x &= (\Delta s/2) \sin \Theta \cos \Phi \\ \Delta y &= (\Delta s/2) \sin \Theta \sin \Phi \\ \Delta z &= (\Delta s/2)(1 + \cos \Theta) ,\end{aligned}\tag{15.18}$$

where  $\Phi$  is a randomly selected azimuthal angle and it is understood that  $\Theta$  is sampled from the Goudsmit-Saunderson [GS40a, GS40b] multiple-scattering theory at the mid-point energy.

Only two previously published Monte Carlo methods have followed this prescription. Berger’s method [Ber63] is similar except that he proposed a straggling term for the lateral components and the energy dependence was taken account for directly. However, the longitudinal and lateral distributions have only been recently been implemented into ETRAN [Sel91].

The other method is the PRESTA algorithm [BR86, BR87] that has been incorporated into EGS. This algorithm is different from Method-3 in that the final longitudinal position was determined by its average rather than the distribution implied by Eq. 15.18. However, this only contributes to the  $O(\Delta s^2)$  error. The other very important distinction is that the PRESTA algorithm employs the Molière multiple-scattering method [Mol47, Mol48] with corrections and limitations discussed by Bethe [Bet53].

There has also been a recently-published method called the Longitudinal and Lateral Correlation Algorithm (LLCA) proposed by Kawrakow [Kaw96a]. It incorporates the Method-3

transport scheme except that the multiple-scattering theory, while representing an improvement over Molière's method is still an approximation [Kaw96b] to the Goudsmit-Saunderson method. However, there is one important improvement over Method-3 in that the lateral position of the electron at the end of the sub-step is connected to the multiple-scattering angle by means of a distribution, rather than direct correlation as implied by Eq. 15.18. For the present, this distribution function has only been calculated using single-scattering methods (analog Monte Carlo or event-by-event elastic scattering). Presumably, this is an  $O(\Delta s^2)$  or higher correction.

### 15.1.2 Physics' step-size constraints

There are also step-size restrictions related to keeping the step-sizes within range of the validity of the theories underlying the condensed history method. This is important, for example, when using the Molière multiple-scattering theory [Mol47, Mol48]. Bethe [Bet53] analyzed Molière multiple-scattering theory, comparing it to the "exact" theory of Goudsmit and Saunderson [GS40a, GS40b] and provided a correction that improves the large-angle behaviour of Molière theory for large angles as Molière theory is couched in the small-angle formalism of Bothe [Bot21] and Wentzel [Wen22]. The electron step-size constraint arises from not allowing the multiple-scattering angle to attain values greater than 1 radian.

Small-angle multiple scattering theories still play an important role in electron Monte Carlo calculations of the Class II variety since Class II condensed history techniques sample the multiple-scattering distributions "on-the-fly" as the pathlength can, in principle be anything within the constraints already discussed. Class I algorithms, as defined in Berger's work [Ber63], demand that the electrons follow a predetermined energy grid, allowing the multiple-scattering distributions to be pre-calculated. While Class I and Class II have their attributes and shortcomings, the use of an approximate multiple-scattering theory in Class II calculations, considered with the conclusion of the previous section, forces the realization that one can not necessarily expect that the limit of small step-size will produce the correct answer for Class-II/approximate multiple-scattering algorithms! It should also be remarked that Class-I/exact multiple-scattering schemes are subject to numerical instabilities as smaller step-sizes require an increasing number of terms in the Legendre series of Eq. 15.11 to be summed. There have been studies demonstrating that one can converge to the incorrect answer in a Class-II/approximate multiple-scattering algorithm [Rog93, Bie96].

Step-size instability of the Molière theory [Mol48] has been studied extensively [AMB93, Bie94] and comparisons with Goudsmit-Saunderson theory [GS40a, GS40b] have been performed [Bet53, Win87] as well as comparisons with single-elastic scattering Monte Carlo [Bie94]. This has motivated the development of a new multiple-scattering theory based on Goudsmit-Saunderson theory [GS40a, GS40b] but formulated in such a way as to allow sampling "on-the-fly" as required by Class II algorithms and eliminating the small step-size numerical instability of the Goudsmit-Saunderson Legendre summation that arises

from the form expressed in Eq. 15.11. This recent work [KB98] will be discussed in a later section. However, this new multiple-scattering theory will guarantee that condensed history Monte Carlo will always converge to the correct answer in the limit of small electron step-size.

### 15.1.3 Boundary step-size constraints

The final category of electron step-size constraint we consider relates to the geometry, specifically interfaces and material boundaries. Although the transport theory expressed in Eq. 15.5 and the various solutions to it describe electron transport in infinite, unbounded uniform media, practical applications contain boundaries and interfaces between media. Except for the stopping of electrons at interfaces and the updating the material-dependent transport data, this problem was not considered until the EGS/PRESTA algorithm was developed [BR86, BR87]. This algorithm requires knowledge of the nearest distance to any interface and shortens the electron step-size accordingly, by setting  $s = s_{\min}^{\perp}$  where  $s_{\min}^{\perp}$  is the nearest distance to any interface. This is always a perpendicular distance (as suggested by the notation) unless the closest distance happens to be along an intersection of two surfaces. This procedure requires more information from the geometry<sup>2</sup> but it is necessary to avoid potential misuse of the underlying transport theory. Of course this shortening can not continue indefinitely as the electron would never reach the surface, a transport equivalent of Xenon's paradox. PRESTA continues the procedure until the transport steps approach the lower limit of validity of Molière theory, usually from about 3 to 20 mean-free-path distances, and then allows the electron to reach the surface, does not model the lateral components of sub-step transport given in Eq. 15.18 (This is a necessary part of the transport logic, otherwise the lateral transport takes the electron away from the surface, in either medium), updates material-dependent data and carries on in the next medium. The initial distance is again related to the lower limit of validity of Molière theory and thereafter the algorithm adjusts step-sizes according to  $s_{\min}^{\perp}$ . As a particle recedes from a boundary, its steps grow and grow, allowing for efficient, rapid transport away from interfaced. This behaviour is depicted in Figure 15.3.

However, this technique is not without its difficulties. Because lateral transport is not modeled for the steps that touch the boundary, the multiple-scattering deflection is performed at the end of the sub-step. Electron can thus backscatter from a surface, requiring careful handling of the transport logic in the vicinity of interfaces [Bie95]. This “boundary-crossing algorithm” as implemented in PRESTA also pushes the Molière theory towards the edge of its region of validity. Granted, the misuse of Molière theory is minimized but it still exists.

---

<sup>2</sup>The general requirements for electron transport in a geometry composed entirely of planar and quadric surfaces (*i.e.* spheroids, cones, hyperboloids, paraboloids) has recently been developed [Bie95]. Although the distance of intersection to any quadric surface along the particle trajectory requires finding the root of a quadratic equation, the nearest distance to a quadric surface is the root of an  $n^{\text{th}}$ -order equation where  $n \leq 6!$



Figure 15.3: This is a depiction of operation of the PRESTA algorithm, which adjusts electron step-sizes in the vicinity of boundaries.

A more fundamental shortcoming was pointed out by Foote and Smyth [FS95] who pointed out that the deflection at the interface can cause a spurious events whereby an electron, having crossed a boundary can assume a trajectory that is parallel, or nearly so, to the surface at this point. The artefact shows up interfaces between condensed materials and gases. An electron penetrating the gas may be scattered into a near-parallel trajectory with the boundary. Even step-sizes of the order of several mean-free-path distances may be too large in the gas.

This artefact can be eliminated through use of a condensed history method that “evaporates” to a single-scattering method in the vicinity of interfaces [Bie96]. The algorithm is sketched in Figure 15.4. Using the new method, the only way that an electron can cross the interface is through a “no scatter drift” across the interface which involves no approximation. This technique, coupled with the new multiple-scattering theory will allow for error-free Monte Carlo calculations in the limit of small step-size in applications with arbitrarily complex geometries, interfaces and media.

## 15.2 The new multiple-scattering theory

The “exact” multiple-scattering angular distribution of Eq. 15.11 may be integrated easily over azimuthal angles (assuming that the cross section does not depend on polarisation) and written:

$$\psi(\cos \Theta, s) = \sum_l (l + 1/2) P_l(\cos \Theta) \exp \left( - \int_0^s ds' \kappa_l(E) \right) , \quad (15.19)$$

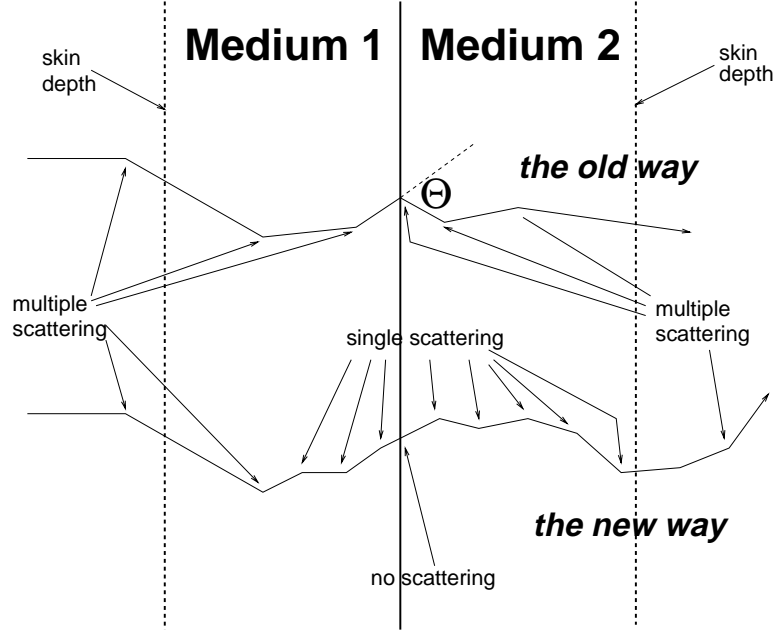


Figure 15.4: This is a depiction of the new boundary-cross algorithm which eliminates boundary-related artefacts.

and then reorganized in the following form [KB98]:

$$\psi(\cos \Theta, s) = e^{-\lambda} \delta(1 - \cos \Theta) + \lambda e^{-\lambda} \tilde{\sigma} + (1 - e^{-\lambda} - \lambda e^{-\lambda}) \sum_l (l + 1/2) P_l(\cos \Theta) \frac{e^{-\lambda g_l} - 1 - \lambda g_l}{e^{-\lambda} - 1 - \lambda}, \quad (15.20)$$

where

$$\lambda = \int_0^s ds' \sigma_s(E) \quad (15.21)$$

is the distance measured in mean-free-path taking into account the change in energy of the scattering cross section, and  $e^{-\lambda}$  is the probability that the electron can go a distance  $\lambda$  without scattering even once,

$$\tilde{\sigma} = \frac{1}{\lambda} \int_0^s ds' \sigma_s(\cos \Theta, E) \quad (15.22)$$

is the angular distribution of a single-scattering event with probability  $\lambda e^{-\lambda}$  taking into account energy loss, and

$$g_l = \frac{1}{\lambda} \int_0^s ds' \int_0^\pi d(\cos \Theta) \sigma_s(\cos \Theta, E) P_l(\cos \Theta), \quad (15.23)$$

which is related to the  $\kappa_l$  defined in Eq. 15.8.

The general form of Eq. 15.21 was suggested by Berger and Wang [BW89] as a way of reducing some of the singularity in Eq. 15.11 to make the summation for large- $l$  tractable.

This approach has some moderate success for Class I pre-calculations but Class II algorithms must still sample “on-the-fly”. Therefore, we have adopted an alternative approach.

This approach is based on a similar analysis of the small-angle multiple-scattering problem [Bie94]. Consider the part of Eq. 15.20 that describes two or more scatterings. Defining the notation

$$\psi^{(2+)}(\mu, s) = \sum_l (l + 1/2) P_l(\mu) \frac{e^{-\lambda g_l} - 1 - \lambda g_l}{e^{-\lambda} - 1 - \lambda}, \quad (15.24)$$

where  $\mu = \cos \Theta$ . The change of variables,

$$u = (1 + a) \left( 1 - \frac{2a}{1 - \mu + 2a} \right) \quad (15.25)$$

allows us to write an alternate form of  $\psi^{(2+)}(\mu, s)$ , namely

$$q^{(2+)}(u, s) du = \psi^{(2+)}(\mu, s) d\mu, \quad (15.26)$$

where for the moment,  $a$  is an arbitrary parameter.

The motivation for this transformation is quite subtle. The magnitude of the derivative of  $u$  with respect to  $\mu$  is:

$$du = (1 + a) \left( 1 - \frac{2a}{1 - \mu + 2a} \right), \quad (15.27)$$

which resembles a screened Rutherford cross section with an arbitrary screening angle,  $a$ . As discovered in the small-angle study, most of the shape of the multiple-scattering distribution, which is peaked strongly in the forward direction for the usual case of small screening angles, resembles a screened Rutherford cross section with some effective width. The “effective screening” angle  $a$  can then be fixed by the requirement that  $q^{(2+)}(u, s)$  be as flat as possible for all angles and all transport distances. The procedure is described elsewhere. It suffices to say that the  $q^{(2+)}$ -surfaces produced, starting with a screened Rutherford cross section employing the Molière screening angle [Mol47] along with Mott [Mot29, Mot32] that includes spin and relativistic corrections [Mot29, Mot32], are flat enough so that a linear interpolation table that is accurate to within 0.2% can be represented in a few hundred kB of data for 100 atomic elements suitable for applications from 1 keV upwards<sup>3</sup>.

## 15.3 Longitudinal and lateral distributions

In this section we consider longitudinal and lateral transport components of Monte Carlo sub-step. Although the transport scheme represented by Eq. 15.18 has been shown to yield results correct to  $O(\Delta s)$ , it can be shown that all the moments represented by Eqs. 15.13–15.17 are not correct. Thus, even average penetration distances and lateral diffusion are not

---

<sup>3</sup>We are grateful to Dr Stephen Seltzer for providing the Mott cross section data.

accounted for correctly. For most applications, electrons scatter for many elastic and inelastic scatterings before tallying some result. After many scatterings, the only information that really matters are the first few moments. There are, of course exceptions, the most important one being low energy electron backscatter. In the application, single and plural events can lead to backscatter from a foil. The “boundary-crossing algorithm” discussed previously may come to the rescue, however. This is because electrons must penetrate using single-scattering methods to a skin-depth of several mean-free-path distances before the condensed history algorithm is allowed to take over. If single and plural scattering from within the skin-depth is contributing in a significant way to the backscatter events, then this will automatically be accounted for.

We now describe a transport algorithm that gives exactly the Lewis moments,  $\langle z \rangle$ ,  $\langle z \cos \Theta \rangle$ ,  $\langle z^2 \rangle$ , and  $\langle x^2 + y^2 \rangle$  with only a little more computational effort<sup>4</sup>.

We create the ansatz:

$$\begin{aligned}\Delta x/s &= [\beta(s) - \delta_{\parallel}(s, \xi_x)] \sin \Theta \cos[\Phi - \delta_{\phi}(s, \xi_{\phi})] + \delta_{\perp}(s, \xi_x) \\ \Delta y/s &= [\beta(s) - \delta_{\parallel}(s, \xi_x)] \sin \Theta \sin[\Phi - \delta_{\phi}(s, \xi_{\phi})] + \delta_{\perp}(s, \xi_y) \\ \Delta z/s &= [\beta(s) - \delta_{\parallel}(s, \xi_z)] \cos \Theta + [\alpha(s) - \delta_{\parallel}(s, \xi_x)] ,\end{aligned}\tag{15.28}$$

where  $\delta_{\perp}$ ,  $\delta_{\parallel}$  and  $\delta_{\phi}$  are transverse, longitudinal and azimuthal straggling functions and  $\xi_i$  is a uniform random variable between 0 and 1. The lateral and longitudinal straggling functions have the property that their average is exactly zero, *i.e.*  $\int_0^1 d\xi \delta_{\perp}(s, \xi) = 0$  and  $\int_0^1 d\xi \delta_{\parallel}(s, \xi) = 0$  while the azimuthal straggling function’s average value represents the average angle between the direction of motion and the azimuthal component of the straggling function [Kaw96a]. It also has a straggling component. This function has been determined by single-scattering calculations [Kaw96a]. The functions  $\alpha(s)$  and  $\beta(s)$  can be found by insisting that  $\langle z \rangle$  and  $\langle z \cos \Theta \rangle$  comply with  $\langle z \rangle$  in Eq. 15.13 and with  $\langle z \cos \Theta \rangle$  in Eq. 15.14. The values of  $\int_0^1 d\xi \delta_{\perp}^2(s, \xi)$  and  $\int_0^1 d\xi \delta_{\parallel}^2(s, \xi)$  can be determined by forcing agreement with  $\langle z^2 \rangle$ , and  $\langle x^2 + y^2 \rangle$ . It should be remarked that the shape of the straggling functions is not determined by this approach. We can derive more information about them by calculating higher Lewis moments. This will lead to information about  $\int_0^1 d\xi \delta_{\perp}^n(s, \xi)$  and  $\int_0^1 d\xi \delta_{\parallel}^n(s, \xi)$ , where  $n > 2$ . Since we do not know the exact shape of the straggling functions, we have to guess. Small-angle theory suggests Gaussian’s for the lateral straggling functions. This work remains to be done. The use of the previously-computed azimuthal straggling function, should guarantee compliance with  $\langle x \sin \Theta \cos \Phi \rangle$  and  $\langle y \sin \Theta \sin \Phi \rangle$ .

Before ending this section, we make a few remarks on the computational efficiency of this new method. The most computationally intensive part of Eq. 15.28 is sampling the multiple-scattering distribution, which is required by any method. The straggling functions can be

---

<sup>4</sup>It is very important remark that more advanced methods have to be computationally efficient. It is pointless to develop complicated calculational schemes that cost more to execute than simply turning down the step-size to obtain the same degree of accuracy!

pre-calculated and put into interpolation tables, a task no more difficult than the multiple-scattering table described in the previous section. Alternatively, since the shape of the distributions is arbitrary, simple forms may be used and sampling these distributions may be very rapid.

One possible criticism of this approach is that it is bound to produce the occasional unphysical result of the form  $x^2 + y^2 + z^s > s^2$ . It is anticipated that this type of event will be rare, and some indication of this has been given by Berger [Ber63], who first suggest Gaussian straggling terms for the lateral component. Another criticism is that the ansatz in Eq. 15.28 is not general enough. Indeed, although moments of the type  $\langle z^n \rangle$  can be used to determine  $\int_0^1 d\xi \delta_{\parallel}^n(s, \xi)$ , they will likely be in conflict with higher order moments of the sort  $\langle z^n \cos^m \Theta \rangle$ . Actually, this criticism is coupled directly to the previous one and results from our incomplete understanding of the solution to the complete transport problem. Further research along these lines, such as the Fokker-Planck solution to this problem, while approximate will shed more insight on the general transport solution. However, it is also likely that Eq. 15.28 represents a significant advance in condensed history methods and may provide true step-size independence for a large class of electron transport problems.

## 15.4 The future of condensed history algorithms

We conclude with some comments on the future of condensed history algorithms to place its research in some sort of larger perspective. We investigate briefly two scenarios that are pointed to by present computer hardware developments. *Will condensed history continue to play a role when computers get much faster?* and *Will analog-based condensation techniques ever replace our analytic-based ones?*

Will condensed history continue to play a role when computers get much faster?

The other was of asking this question is: *Will analog Monte Carlo techniques replace condensed history methods for most future applications?*

Depending on the application, condensed history techniques “outrun” single-scattering calculations by a factor  $10^3$ – $10^5$ . Computing power per unit cost increases by approximately a factor of 2 every year. This means that an application that runs today with condensed history calculations can be done in the same amount of time by analog methods in about 10–17 years!

The answer to this is that the problems usually expand in complexity as the technology to address them advances. In the next decade or two we will not be asking the same questions! The questions will be more complex and the simpler, cruder method of condensed history, whatever it evolves to in that time, will still have an important role to play.

A perfect example of this is radiotherapy treatment planning calculations. Presently, condensed history techniques are not used because it takes a few hours to perform on a workstation-

class computer. Software and hardware technology may reduce this to seconds in about 5 years, making it feasible for routine use. In a few more years, calculation times will be microseconds and Monte Carlo will be used in all phases of treatment planning, even the most sophisticated such as inverse planning and scan-plan-treat single pass tomotherapy machines.

Condensed history gets this answer to sufficient accuracy and medical physics will not resort to single-scattering methods that take  $10^3$ – $10^5$  longer to execute for marginal (and and largely unnecessary) gain in accuracy. Once calculation error has been reduced to about 2% or so, its contribution to the overall error of treatment delivery will be negligible.

Will analog-based condensation techniques ever replace our analytic-based ones?

One approach to addressing the problem of slow execution for single-scattering Monte Carlo is to pre-compute electron single-scattering histories and tally the emergence of particles from macroscopic objects of various shapes, depending on the application. Then one transports these objects in the application rather than electrons! Ballinger *et. al.* [BRM92] used hemispheres as his intended application was primarily low-energy backscatter from foils. Ballinger *et. al.* did their calculations within the hemispheres almost completely in analog mode, for both elastic and inelastic events.

Neuenschwander and Born [NB92] and later Neuenschwander *et. al.* [Nel95] used EGS4 [NHR85, BHNR94] condensed history methods for pre-calculation in spheres for the intended application of transport within radiotherapy targets (CT-based images) and realized a speed increase of about 11 over condensed history. Svatos *et. al.* [SBN<sup>+</sup>95] is following up on this work by using analog methods.

Since these “analog-based condensation” techniques play a role in specialized applications it begs the question whether or not these techniques can play a more general role. To answer this, consider that we are seeking the general solution to the problem: given an electron starting at the origin directed along the  $z$ -axis for a set of energies  $E_n$ , what is the complete description of the “phase space” of particles emerging from a set spheres<sup>5</sup> of radii  $r_n$ ? That is, what is  $\psi(\vec{x}, \vec{\Omega}, E, s, q; E_n, r_n)$ , where  $\vec{x}$  is the final position on the sphere,  $\vec{\Omega}$  is the direction at the exit point of the sphere,  $E$  is the exit energy,  $s$  is the total pathlength,  $q$  is the charge (3 possible values in our model, electrons, positrons or photons),  $E_n$  is the starting energy, and  $r_n$  is the radius of the sphere. Now, imagine that we require  $n$ -points to fit some input or output phase-space variable (*e.g.* 100 different values of  $E$ ) and that we must provide storage for  $N$  decades of input energy. (The input and output energies would likely be tabulated on a logarithmic mesh.) The result is that one would require  $3Nn^8$  real words of data to store the results of the general problem!

To make the example more concrete, imagine that we wish to store 9 decades in input energy (from, say, 1 keV to 100 TeV) and set  $n = 100$ . This would require 1.2 exabytes ( $1.2 \times 10^{18}$ )

---

<sup>5</sup>We will use this geometry as an example. A set of spheres is necessary so that geometry-adaptive techniques may be employed.

bytes of information. Estimating current on-line storage capability at about 10 terabytes/m<sup>3</sup>, the required storage would be  $1.2 \times 10^5$  m<sup>3</sup>, or a cube about 50 m on a side. This class of solution would require storage densities of the order  $10^2$ – $10^3$  greater than current technology, something for the distant future, perhaps in 50 years or so?

However, this solution really reflects a paucity of clever ideas. In a previous section we have already seen how multiple-scattering angles can be represented compactly. It is likely that further research may give us more insight into how to represent the data to the entire problem in a compact way. It may turn out that the future of this class of Monte Carlo calculations may be with pre-computed distributions. However, condensed history research will provide the most sensible way to *interpolate* the data. The better the interpolation scheme, the more compact the data will be. This may be the surviving contribution of condensed history research in the distant future.



# Bibliography

- [AMB93] P. Andreo, J. Medin, and A. F. Bielajew. Constraints on the multiple scattering theory of Molière in Monte Carlo simulations of the transport of charged particles. *Med. Phys.*, 20:1315 – 1325, 1993.
- [Ber63] M. J. Berger. Monte Carlo Calculation of the penetration and diffusion of fast charged particles. *Methods in Comput. Phys.*, 1:135 – 215, 1963.
- [Bet53] H. A. Bethe. Molière’s theory of multiple scattering. *Phys. Rev.*, 89:1256 – 1266, 1953.
- [BHNR94] A. F. Bielajew, H. Hirayama, W. R. Nelson, and D. W. O. Rogers. History, overview and recent improvements of EGS4. *National Research Council of Canada Report PIRS-0436*, 1994.
- [Bie94] A. F. Bielajew. Plural and multiple small-angle scattering from a screened Rutherford cross section. *Nucl. Inst. and Meth.*, B86:257 – 269, 1994.
- [Bie95] A. F. Bielajew. HOWFAR and HOWNEAR: Geometry Modeling for Monte Carlo Particle Transport. *National Research Council of Canada Report PIRS-0341*, 1995.
- [Bie96] A. F. Bielajew. A hybrid multiple-scattering theory for electron-transport Monte Carlo calculations. *Nucl. Inst. and Meth.*, B111:195 – 208, 1996.
- [Bot21] W. Bothe. Das allgemeine Fehlergesetz, die Schwankungen der Feldstärke in einem Dielektrikum und die Zerstreung der  $\alpha$ -Strahlen. *Z. für Physik*, 5:63 – 69, 1921.
- [BR86] A. F. Bielajew and D. W. O. Rogers. PRESTA: The Parameter Reduced Electron-Step Transport Algorithm for electron Monte Carlo transport. *National Research Council of Canada Report PIRS-0042*, 1986.
- [BR87] A. F. Bielajew and D. W. O. Rogers. PRESTA: The Parameter Reduced Electron-Step Transport Algorithm for electron Monte Carlo transport. *Nuclear Instruments and Methods*, B18:165 – 181, 1987.

- [Bri86] J. Briesmeister. MCNP—A general purpose Monte Carlo code for neutron and photon transport, Version 3A. *Los Alamos National Laboratory Report LA-7396-M (Los Alamos, NM)*, 1986.
- [Bri93] J. F. Briesmeister. MCNP—A general Monte Carlo N-particle transport code. *Los Alamos National Laboratory Report LA-12625-M (Los Alamos, NM)*, 1993.
- [BRM92] C. T. Ballinger, J. A. Rathkopf, and W. R. Martin. The response history Monte Carlo method for electron transport. *Nucl. Sci. Eng.*, 112:283 – 295, 1992.
- [BW89] M. J. Berger and R. Wang. Multiple-scattering angular deflections and energy-loss straggling. In T.M. Jenkins, W.R. Nelson, A. Rindi, A.E. Nahum, and D.W.O. Rogers, editors, *Monte Carlo Transport of Electrons and Photons*, pages 21 – 56. Plenum Press, New York, 1989.
- [FS95] B. J. Foote and V. G. Smyth. The modeling of electron multiple-scattering in EGS4/PRESTA and its effect on ionization-chamber response. *Nucl. Inst. and Meth.*, B100:22 – 30, 1995.
- [GS40a] S. A. Goudsmit and J. L. Saunderson. Multiple scattering of electrons. *Phys. Rev.*, 57:24 – 29, 1940.
- [GS40b] S. A. Goudsmit and J. L. Saunderson. Multiple scattering of electrons. II. *Phys. Rev.*, 58:36 – 42, 1940.
- [HKM<sup>+</sup>92] J. A. Halbleib, R. P. Kensek, T. A. Mehlhorn, G. D. Valdez, S. M. Seltzer, and M. J. Berger. ITS Version 3.0: The Integrated TIGER Series of coupled electron/photon Monte Carlo transport codes. *Sandia report SAND91-1634*, 1992.
- [Kaw96a] I. Kawrakow. Electron transport: longitudinal and lateral correlation algorithm. *Nuclear Instruments and Methods*, B114:307 – 326, 1996.
- [Kaw96b] I. Kawrakow. Electron transport: multiple and plural scattering. *Nuclear Instruments and Methods*, B108:23 – 34, 1996.
- [KB98] I. Kawrakow and A. F. Bielajew. On the representation of electron multiple elastic-scattering distributions for Monte Carlo calculations. *Nuclear Instruments and Methods*, B134:325 – 336, 1998.
- [Lar92] E. W. Larsen. A theoretical derivation of the condensed history algorithm. *Ann. Nucl. Energy*, 19:701 – 714, 1992.
- [Lew50] H. W. Lewis. Multiple scattering in an infinite medium. *Phys. Rev.*, 78:526 – 529, 1950.

- [Mol47] G. Z. Molière. Theorie der Streuung schneller geladener Teilchen. I. Einzelstreuung am abgeschirmten Coulomb-Feld. *Z. Naturforsch.*, 2a:133 – 145, 1947.
- [Mol48] G. Z. Molière. Theorie der Streuung schneller geladener Teilchen. II. Mehrfach- und Vielfachstreuung. *Z. Naturforsch.*, 3a:78 – 97, 1948.
- [Mot29] N. F. Mott. . *Proc. Royal Society London*, A124:425, 1929.
- [Mot32] N. F. Mott. . *Proc. Royal Society London*, A135:429, 1932.
- [NB92] H. Neuenchwander and E. J. Born. A Macro Monte Carlo method for electron beam dose calculations. *Phys. Med. Biol.*, 37:107 – 125, 1992.
- [Nel95] W. R. Nelson. private communication. (*conversation with A.F. Bielajew*), 1995.
- [NHR85] W. R. Nelson, H. Hirayama, and D. W. O. Rogers. The EGS4 Code System. Report SLAC-265, Stanford Linear Accelerator Center, Stanford, Calif, 1985.
- [Rog84] D. W. O. Rogers. Low energy electron transport with EGS. *Nucl. Inst. Meth.*, 227:535 – 548, 1984.
- [Rog93] D. W. O. Rogers. How accurately can EGS4/PRESTA calculate ion chamber response? *Medical Physics*, 20:319 – 323, 1993.
- [SBN<sup>+</sup>95] M. M. Svatos, C. T. Ballinger, H. Neuenchwander, T. R. Mackie, W. P. Chandler, C. L. Hartmann-Siantar, J. A. Rathkopf, and P. J. Reckwerdt. Electron transport in radiotherapy using local-to-global Monte Carlo. In “*Proceedings of the International Conference on Mathematics and Computations, Reactor Physics, and Environmental Analyses*” (American Nuclear Society Press, La Grange Park, Illinois, U.S.A.), pages 154 – 161, 1995.
- [Sel89] S. M. Seltzer. An overview of ETRAN Monte Carlo methods. In T.M. Jenkins, W.R. Nelson, A. Rindi, A.E. Nahum, and D.W.O. Rogers, editors, *Monte Carlo Transport of Electrons and Photons*, pages 153 – 182. Plenum Press, New York, 1989.
- [Sel91] S. M. Seltzer. Electron-photon Monte Carlo calculations: the ETRAN code. *Int'l J of Appl. Radiation and Isotopes*, 42:917 – 941, 1991.
- [Wen22] G. Wentzel. Zur theorie der streuung von  $\beta$ -strahlen. *Ann. Physik*, 69:335 – 368, 1922.
- [Win87] K. B. Winterbon. Finite-angle multiple scattering. *Nuclear Instruments and Methods*, B21:1 – 7, 1987.